Astronomy & Astrophysics manuscript no. draft
October 7, 2016
©ESO 2016

Stable laws and cosmic ray physics

Y. Genolini*, P. Salati, P. D. Serpico, and R. Taillet

LAPTh, Université Savoie Mont Blanc & CNRS, 9 Chemin de Bellevue, B.P.110 Annecy-le-Vieux, F-74941, France

Received; accepted
Preprint numbers : LAPTH-045/16

ABSTRACT

Context. In the new "precision era" for cosmic ray astrophysics, theoretical predictions cannot content themselves with average trends, but need to correctly take into account intrinsic uncertainties. The space-time discreteness of the cosmic ray sources, joined with a substantial ignorance of their precise epochs and locations (with the possible exception of the most recent and close ones) plays an important role in this sense.
Aims. We elaborate a statistical theory to deal with this problem, relating the composite probability $P(\Psi)$ to obtain a flux Ψ at the Earth to the single-source probability $p(\psi)$ to contribute with a flux ψ. The main difficulty arises since $p(\psi)$ is a "heavy tail" distribution, characterized by power-law or broken power-law behaviour up to very large fluxes for which the central limit theorem does not hold, and leading to *stable laws* as opposed to Gaussian distributions.
Methods. We discuss analytically the regime of validity of the stable laws associated to the distributions arising in cosmic ray astrophysics, as well as the limitations to the treatment imposed by causal considerations and partial source catalogue knowledge. We validate our results with extensive Monte Carlo simulations, for different regimes of propagation parameters and energies.
Results. We find that relatively simple recipes provide a satisfactory description of the probability $P(\Psi)$. We also find that a naive Gaussian fit to simulation results would underestimate the probability of very large fluxes, i.e. several times above the average, while overestimating the probability of relatively milder excursions. At large energies, large flux fluctuations are prevented by causal considerations, while at low energies a partial knowledge on the recent and nearby population of sources plays an important role. A few proposal have been recently discussed in the literature to account for spectral breaks reported in cosmic ray data in terms of local contributions. We apply our newly developed theory to assess their probabilities, finding that they are relatively small, typically at the 0.1% level or smaller, never exceeding 1%.
Conclusions. The use of heavy tail distributions is relevant in assessing how likely a measured cosmic ray flux departs from the average expectation in a given model. The existing mathematical theory leading to stable laws can be adapted to the case of interest via some recipes relatively easy to implement and that closely reproduce numerical simulations.

Key words. Astroparticle physics - cosmic rays - local sources - statistical methods

arXiv:1610.02010v1 [astro-ph.HE] 6 Oct 2016

1. Introduction

A striking property of the (Galactic) cosmic ray spectra is their power-law behaviour over many decades in energy. Power laws are omnipresent in nature (as well as in many domains of interest for human activities), typically associated to self-similar/scale invariant phenomena. For instance, the photon spectra—thought to be tracers of the parent charged cosmic ray particle spectra—of most sources in high-energy astrophysics (supernova remnants, pulsar wind nebulae, diffuse radiations, etc.) at different wavelengths, from radio to gamma-rays, are also well described by (broken) power laws, typically with spectral index α in a relatively narrow range $-3 < \alpha < -1$. Even the interstellar magnetic field turbulence is well-described by a power-law power spectrum, which in turn justifies a power-law behaviour for the rigidity dependence of the diffusion coefficient describing cosmic ray propagation in the Galaxy.

Not surprisingly, then, the customary calculation of the cosmic ray flux at the Earth postulates a universal power-law source term, further assuming the limit of a continuous distribution of sources, both spatially and temporally, in a volume modelling the Galaxy: often, a simple cylinder or an effectively infinite slab. This is an approximation, as the distribution of cosmic ray sources is actually discrete. This approximation is valid if the distribution of sources is sufficiently dense in space and in time to be described as a continuum, much like in thermodynamics when the details of microscopic states corresponding to a given macroscopic state are ignored. This approximation makes perfect sense to describe the average expectations for the flux at Earth associated to a given hypothesis on propagation parameters and source spectra and energetics. However, the discrete nature of cosmic ray sources should affect other observables, for instance the time variation of the flux measured, which are nonetheless less important for all but a few phenomenological consequences.

Indeed, recently several experiments have established that the cosmic ray spectrum, even within the three decades of energy probed by a single experiment like AMS-02, cannot be satisfactorily described by a single power-law (for a recent review see Sec. 2

*Contact author: yoann.genolini@lapth.cnrs.fr

in Serpico (2015)). This is observed for protons, helium nuclei and some heavier species. Several articles have attempted to explain this phenomenology as the result of the discrete nature of cosmic ray sources in space and time (as reviewed in Sec. 3.3 of Serpico (2015) and also in Bernard et al. (2012)). While specific scenarios fitting the data can be found, the crucial question (how *likely* are these solutions, given our statistical knowledge of the source distribution and rate?) is typically left unanswered. This is related to the conceptual difficulty that the probability distribution function p of a single source contributing a flux ψ at Earth is not a Gaussian function, rather a heavy-tail/power law distribution which, if extrapolated to very large fluxes, does not even have a finite variance: the central limit theorem for the sum flux probability distribution $P(\Psi)$ cannot be applied. Ironically, the same mathematical property that makes a phenomenological description of the cosmic ray observables so simple ("power laws") raises difficulties in theoretical probabilistic assessments starting from $p(\psi)$! While this problem has been clearly recognized (Lee 1979; Lagutin & Nikulin 1995), the quantitative consequences of this fact for cosmic ray physics are still a matter of debate. Far from being academic, the problem has also important implications for the theoretical limitations in the extraction of propagation parameters, as well as comparing theoretical models up to current experimental precision. Ultimately, barring an unrealistic, fully deterministic model of the sources of cosmic rays, theoretical predictions in this field are intrinsically statistical in nature.

Here, we aim at establishing a systematic theory to evaluate these effects. Our main focus is on analytical treatment, but all major conclusions are validated by extensive numerical simulations. Also, compared with previous literature in this domain, we analyse the effects of physical limitations on idealized mathematical extrapolations, such as the eventual failure of diffusion equations to cope with constraints such as causality or a priori knowledge about the discrete source distribution. Whenever a comparison with observations is performed, we will refer to the proton flux, which is the best measured one due to high statistics, and for which the effects discussed here should be most prominent. Still, the same formalism can apply to any nuclear species, and could also be extended to leptons (at least qualitatively).

As an application, we then focus on the compatibility of several experimental results on interstellar protons (such as AMS-02, Pamela, CREAM) with our current understanding of cosmic ray propagation, properly taking the theoretical uncertainty into account.

This paper is organised as follows. In Sec. 2 we describe the problem and introduce the main difficulties which make its solution challenging, as well as our strategy to attack them. Section 3 deals with the technical aspects of the analytical treatment proposed, including a discussion of the limitations of a too naive approach. Section 4 compares the theory with extensive simulations. A few applications to cases of interest are reported in Sec. 5. Finally, in Sec. 6 we conclude.

2. Setting of the problem

Galactic cosmic rays are accelerated at discrete sources, the position and age of which is not known individually, only statistically. From the statistical distribution of these sources, we can infer the statistical distribution of the cosmic ray flux in the solar neighbourhood. In this section, we describe the issues raised by this program. The cosmic ray (CR) flux Ψ obeys a diffusion equation which, in its simplest incarnation [1], boils down to the form (energy dependence implicit):

$$\left[\frac{\partial}{\partial t} - K\,\nabla^2\right]\Psi = Q\,, \tag{1}$$

where K is the spatial diffusion coefficient and Q is the source term. The solution to this equation can be formally written as an integral over the Galactic volume and over the past Galactic history as:

$$\Psi(\mathbf{x},t) = \int_{-t_{\rm MW}}^{t} dt_S \int_{V_{\rm MW}} d\mathbf{x}_S\; Q(\mathbf{x}_S,t_S)\; \mathcal{G}_B(\mathbf{x}_S,t_S \rightarrow \mathbf{x},t)\,, \tag{2}$$

where $V_{\rm MW}$ is the volume of the Galaxy, given by $V_{\rm MW} \simeq 2\,h\,\pi\,R^2$ if the Galaxy is modeled as a cylinder of radius R and half-thickness h, of age $t_{\rm MW}$, and $\mathcal{G}_B$ is the Green function, obtained by solving the analogous of Eq. (1) with a temporal and spatial delta at the RHS, and the appropriate boundary conditions. For reminder, the Green function of the pure diffusive problem (without boundary) with delta centered at spatial position $\boldsymbol{x_S}$ and time t_S would simply writes

$$\mathcal{G}(d=|\boldsymbol{x}-\boldsymbol{x_S}|,\tau=t-t_S) = \frac{1}{(4\,\pi\,K\,\tau)^{3/2}}\exp\left(-\frac{d^2}{4\,K\,\tau}\right). \tag{3}$$

There are a few issues related to the computation of the CR flux, which we now sketch.

First, the source term Q is expected to be a sum of discrete injection points in space-time (the spatial and time scale of likely accelerators being assumed much shorter than propagation length and time), whose actual positions and epochs are unknown. This is the so-called myriad model approach (Higdon & Lingenfelter 2003) where cosmic rays are sourced by a constellation of point-like objects and not by a continuous jelly. It would then be formally correct to write

$$Q(\mathbf{x}_S,t_S) = \sum_i^N q_i\;\delta(\boldsymbol{x_i}-\boldsymbol{x}_S)\;\delta(t_i-t_S)\,, \tag{4}$$

[1] The diffusion coefficient K is supposed to be uniform in the diffusion volume. Additional terms accounting for convection, reacceleration and energy losses are of little relevance for the species and the energy ranges of interest in the following.

leading to

$$\Psi(\mathbf{x},t) = \sum_i^N \psi_i = \sum_i^N q_i \, \mathcal{G}_B(\mathbf{x}_i, t_i \rightarrow \mathbf{x}, t) \, . \tag{5}$$

What is usually done is to replace Eq. (1), sourced by a discrete sum, with a continuous proxy corresponding to its ensemble average. In particular the source term writes (for simplicity we assume a unique source term, i.e. $q_i = q$):

$$\langle Q(\mathbf{x}_S, t_S) \rangle = \left\langle \sum_i^N q_i \, \delta(\boldsymbol{x_i} - \boldsymbol{x}_S) \, \delta(t_i - t_S) \right\rangle \simeq \frac{q\,\nu}{V_{\rm MW}} \times \begin{cases} \Theta(h - |z|)\,\Theta(R - r) & \text{in 3D, or} \\ \\ 2h\,\delta(z)\,\Theta(R - r) & \text{in 2D,} \end{cases} \tag{6}$$

where q is the single source spectrum (particles per unit energy) and ν the source rate per unit time. For instance, assuming supernova remnants to be the sources of CRs, a rate of 3 explosions per century is reasonable. In the second equality, we assume a homogeneous distribution of sources lying within a cylindrical approximation of the Galaxy with radius R. Along the vertical direction the sources are either uniformly distributed inside a disk with half-thickness h (3D case), or pinched inside an infinitely thin disk (2D case). The generalization to a different distribution is straightforward.

This source term leads to the theoretical average flux:

$$\langle \Psi(\mathbf{x},t) \rangle = \int_{-t_{\rm MW}}^{t} dt_S \int_{V_{\rm MW}} d\mathbf{x}_S \; \langle Q(\mathbf{x}_S, t_S) \rangle \, \mathcal{G}_B(\mathbf{x}_S, t_S \rightarrow \mathbf{x}, t) \, . \tag{7}$$

This is only true on average. We expect the flux observed at the Earth to be ruled by a probability distribution function (pdf) $P(\Psi)$. This function also depends on the actual value of N of the underlying discrete sources. The average flux becomes

$$\langle \Psi \rangle = \int_0^\infty d\Psi \, \Psi \, P(\Psi) \, . \tag{8}$$

Obtaining the probability $P(\Psi)$ entering e.g. in Eq. (8) requires a "change of variables", from space-time location to flux space. To this purpose, we exploit the fact that there is a straightforward relation between $\{t_S, \mathbf{x}_S\}$ and the flux obtained by a single source, ψ_S, located at $\{t_S, \mathbf{x}_S\}$. For example, Eq. (8) can be rewritten in terms of the pdf for the flux from a single source, $p(\psi)$, as

$$\langle \Psi \rangle = \int_0^\infty d\Psi \, \Psi \, P(\Psi) \; = N \langle \psi \rangle = N \int_0^\infty d\psi \, \psi \, p(\psi) \, . \tag{9}$$

Obtaining $p(\psi)$ (or rather its cumulative distribution) is the main subject of Sec. 3.2. Let us just note that the link is formally written as

$$p(\psi, \boldsymbol{x}, t) = \frac{\nu}{N \, V_{\rm MW}} \int_{-t_{\rm MW}}^{t} dt_S \int_{\rm V_{MW}} d\mathbf{x}_S \; \delta(\psi - q \, \mathcal{G}_B(\mathbf{x}_S, t_S \rightarrow \mathbf{x}, t)) \, . \tag{10}$$

Once $p(\psi)$ is known, the pdf for the sum flux is formally written as

$$P(\Psi) = \int_{\psi_1} \int_{\psi_2} \ldots \int_{\psi_N} p(\psi_1) \; p(\psi_2) \ldots p(\psi_N) \; \delta\left(\sum_i^N \psi_i - \Psi \right) \, {\rm d}\psi_1 {\rm d}\psi_2 .. {\rm d}\psi_N \; . \tag{11}$$

This relation is based on the disputable yet natural assumption that the sources are not correlated with each other. The probability that two sources yield respectively the fluxes ψ_1 and ψ_2 is thus given by the product $p(\psi_1) \; p(\psi_2)$.

Here comes the second difficulty: if we try to use the generalization of Eq. (9) to compute, say, the second moment of the flux, $\langle \Psi^2 \rangle$, and hence the expected variance of the flux, the expression formally diverges since the underlying $p(\psi)$ has a power-law tail, $p(\psi) \propto \psi^{-\alpha-1}$, with $1 < \alpha < 2$ (see also (Bernard et al. 2012)). It turns out that despite the fact that (for instance) the variance of $p(\psi)$ is formally infinite, thanks to a so-called *generalized* central limit theorem, the resulting probability $P(\Psi)$, for large N, has a universal shape, a so-called *stable law*, only dependent on α and independent of N, but for a rescaling. More details on this will be given in Sec. 3.1. Hence this difficulty does not appear so severe, since meaningful statistical quantities (such as confidence levels or quantiles) can be still computed in this limit. A relatively minor complication is that the index α of the pdf $p(\psi)$ is in fact energy dependent and depends on the propagation model as well. We shall introduce in Sec. 3.2 two limiting behaviours of α which allow for a satisfactory description of the distribution over a wide range of fluxes.

The third issue is that some of the above-mentioned properties depend on the fact that the behaviour $p(\psi) \propto \psi^{-\alpha-1}$ formally extends to infinity. Physically, however, there is no such a thing as an infinite flux: an obvious cutoff is imposed for instance by the empirically established absence of a source too close and/or too recent; of course, this depends on the level of credibility attributed to independent astrophysical information, such as available catalogues. In Sec. 3.3 and Sec. 3.5 we will see what is the impact of this constraint on the maximum flux. A more subtle reason why there is an effective cutoff to the domain of the probability distribution function $p(\psi)$ is the fact that Eq. (1) is non-relativistic, and does not automatically ensure that causality is fulfilled. Accounting exactly for this is outside of the scopes of our treatment, but we will show that this introduces an effective cutoff which is particularly relevant at high energies (see Sec.s 3.3 and 3.4). In either case, however, the conceptual problem that arises is that

for a pdf $p(\psi)$ with a finite support, the asymptotic pdf for the sum of the fluxes variable Ψ is now a Gaussian, due to the standard central limit theorem (moments are in fact finite). It turns out that stable laws still provide acceptable descriptions of the pdf $P(\Psi)$ up to the fluxes of phenomenological interests, and that for the values of N and Ψ of actual interest one is quite far from the Gaussian limit and much closer to the stable law limit. This aspect will be described in Sec. 3.3.

Before concluding this Section, a couple of comments are in order.

First, we shall limit ourselves to discuss the probabilities of departures of fluxes from their average only at a single energy. A natural generalization would be to discuss the probability that the flux at the Earth departs from its expected average value by more than a certain amount at two or more energies. Fluxes at different energies (especially near ones) are not expected to be independent, rather strongly correlated, which can be formally described for instance via the following inequality in the conditional probability

$$P([\Psi(E_1) > \langle\Psi(E_1)\rangle] \cap [\Psi(E_2) > \langle\Psi(E_2)]\rangle) \neq P(\Psi(E_1) > \langle\Psi(E_1)\rangle)\, P(\Psi(E_2) > \langle\Psi(E_2)\rangle)\,. \tag{12}$$

A manifestation of this property if second moments are finite is

$$\langle\Psi(E_1)\Psi(E_2)\rangle \neq \langle\Psi(E_1)\rangle\langle\Psi(E_2)\rangle\,. \tag{13}$$

Estimating the probability of the most significant deviation among the different energy bins provides however an upper limit to the true probability of observing the actual flux excursion at different energy bins, the former being necessarily equal or lower due to the unitarity property of pdfs.

Second, while the effects discussed in our paper are the result of replacing the true underlying discrete source distribution with a continuum space-time distribution which describes its smooth average, and are thus accounting for the partial (only "probabilistic") knowledge we have on the sources frequency and position, this is different from what is usually intended via the "effects of the granularity" of the sources, e.g. in statistical mechanics. These would typically manifest themselves in higher order correlation functions (again, if finite, otherwise via conditional probabilities), like the correlations of fluxes measured at different times, or at the same time at different locations, etc. We emphasize that all source explosions models sharing the same time and volume average would give us the same flux $\langle\Psi\rangle$, while the above higher order correlation observables could be different. In particular in the myriad model approach which we follow here, we assume point-like sources not to be correlated with each other. For example, a model where 20 SN explode randomly in the Galaxy every 800 years, but together at the same time, does not satisfy this condition, and will yield a different probability distribution function (PDF) $P(\Psi)$ for the flux than a model where 1 SN explodes randomly in the Galaxy every 40 years. Both models have the same average flux but fluctuations around that mean do not follow the same law, and for instance time correlations are different. On the other hand, our formalism can still provide a good approximation of strongly correlated source models: if the sources are strongly correlated in space and time (say, the 20 SN in the example above were to explode within a few pc distance of one another), just downscaling ν and increasing q by a corresponding factor would provide a satisfactory approximation for all but very small scale correlations.

3. Technical aspects

3.1. Generalized Central Limit Theorem: Mathematical statement

The central limit theorem states that the sum Ψ of a large number N of independent, identical and stochastic variables ψ is distributed according to a Gaussian law whose variance σ^2_Ψ is N times larger than the variance σ^2_ψ of each individual contribution ψ. In our case though, the pdf of ψ has a power-law tail $p(\psi) \propto \psi^{-\alpha-1}$ with $1 < \alpha < 2$. The average flux $\langle\psi\rangle$ from a single source is defined but not its variance and the central limit theorem cannot be applied, at least in its mundane version.

A more general form of the theorem has been discussed e.g. in section 1.8 of Nolan (2012) and can be readily applied to our problem. We just recall here the salient features of the version that can be adapted to the myriad model. Let ψ be a random variable with probability law $p(\psi)$ defined on $\mathbf{R}_+$. The tail behaviour can be captured by the cumulative distribution function (also called survival function) $C(\psi)$ such that

$$\forall\psi \geqslant 0, \quad C(\psi) \equiv \int_\psi^\infty p(\psi')\,\mathrm{d}\psi'\,. \tag{14}$$

That function encodes the probability for the flux of a single source to be larger than ψ. As shown in what follows, its asymptotic behaviour, which turns out to be an essential ingredient in the proof of the generalized theorem, has the simple power-law form

$$\lim_{\psi\to\infty} \psi^\alpha C(\psi) = \eta > 0\,. \tag{15}$$

We denote by $\Psi = \psi_1 + \cdots + \psi_N$ the sum of N independent and identically p distributed random variables ψ_i. By introducing the rescaled flux

$$S_N = \frac{\Psi - \langle\Psi\rangle}{\sigma_N}, \quad \text{with} \quad \sigma_N = \left(\frac{\eta\,\pi\,N}{2\Gamma(\alpha)\sin(\alpha\,\pi/2)}\right)^{1/\alpha}, \tag{16}$$

the generalized central limit theorem states that the probability law P of S_N converges for large N toward the peculiar stable law $\mathbf{S}[\alpha, 1, 1, 0; 1]$, in the notation of Nolan (2012). Note that the spread parameter σ_N of the stable law depends on the constant η and increases as $N^{1/\alpha}$ instead of $\sqrt{N}$ in the gaussian case. The general stable law function $\mathbf{S}[\alpha, \beta, \gamma, \delta; 1]$ also depends on additional arguments beyond the stability index α, notably a skewness parameter β, a scale parameter γ, and a location parameter δ. The last

index sets the type of parameterization used, as several ones exist in the literature. For instance, the normal or Gaussian distribution centered around μ and with variance σ^2 is denoted in this notation as $\mathbf{N}(\mu, \sigma) = \mathbf{S}(2, 0, \sigma/\sqrt{2}, \mu; 1)$. We recall that a pdf that is invariant under the product of convolution is called stable. This is the case for well-known examples such as the Gaussian, Cauchy and Lévy distributions. But this class of functions is broad, as shown by Paul Lévy in his study of sums of independent identically distributed terms in the 1920's (Lévy 1925). Most of the densities and distribution functions which it encompasses cannot be expressed analytically by closed-form expressions, although their Fourier transforms are tractable. That is why stable laws, such as the Pareto-Levy distribution $\mathbf{S}[\alpha, 1, 1, 0; 1]$ which we use herefater, are not common in the field of astrophysics, but are quite well known in finance for instance (Mandelbrot 1960; Uchaikin & Zolotarev 1999). Nowadays, computer programs such as Mathematica (Wolfram Research, Inc. 2016) can be easily used to compute these special functions.

3.2. Application of the theorem to the probability of measuring a Galactic CR flux

To compute the spread σ_N that comes into play in the stable law followed by the total flux Ψ_N, we need to determine the spectral index α so that $\lim_{\psi\to\infty} C(\psi)\ \psi^\alpha = \eta$. We recall that $C(\psi)$ is the survival probability to get at the Earth a flux higher than ψ. This probability can be obtained by integrating the density of a single source in space and time over the phase space region where it produces a flux larger than ψ.

As we are interested in the limit where the flux ψ is large, if not infinite, the source must be local and young. In that case, CR propagation is the same as if the magnetic halo was infinite and diffusion was dominating the other processes such as convection and spallation. The region in space and time that yields a flux ψ may be derived from the boundless propagator of Eq. (3) which we translate into:

$$\psi = \frac{a}{\tau_M^{3/2}}\, x^{-3/2} \exp\left(-\frac{d^2}{4K\tau_M\, x}\right), \quad \text{with} \quad a = \frac{q}{(4\pi K)^{3/2}}\ . \tag{17}$$

For simplicity we have introduced the dimensionless time variable $x \equiv \tau/\tau_M$, where the timescale τ_M is defined as the maximal age for a source to provide a flux ψ. That value is reached when the source is located at $r = 0$ and is equal to $\tau_M = (a/\psi)^{2/3}$. It is straightforward to check that, for a given value K of the diffusion coefficient, and hence at a given CR energy E, all space-time points in the plane (x, d^2) satisfying the condition

$$\frac{d^2}{6\,K\,\tau_M} = -x \ln x \tag{18}$$

are characterized by the same flux $\psi \equiv \psi(r = 0, \tau = \tau_M)$. This corresponds to the thick blue line drawn in Fig. 1. Points below that curve yield a flux $\psi' > \psi(0, \tau_M)$, while points above it produce a flux $\psi' < \psi(0, \tau_M)$. One can thus compute the cumulative

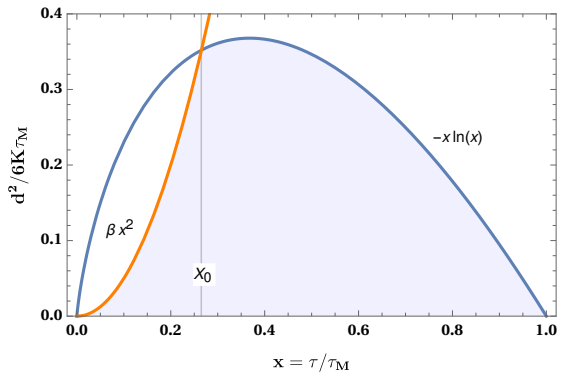

Fig. 1. Below the thick line: space and time region where a source contributes a flux $\psi' > \psi = a/\tau_M^{3/2}$ in the diffusion approximation. Light blue shaded region: space and time domain which also respects the causal constraint.

distribution $C(\psi)$ (sources with fluxes larger than ψ) by integrating the space and time density distribution of a single source $\rho(\boldsymbol{r}, t)$ (assumed constant in the following) over the region in phase space located below the blue line of Fig. 1. In the cylindrical approximation, denoting by N the number of sources contributing to the total flux Ψ allows us to write:

$$\rho(\boldsymbol{r}, t) = \frac{\nu}{2\,h\,\pi\,R^2}\,\frac{1}{N}\ . \tag{19}$$

There is no closed-form expression for $C(\psi)$ in general, but two relevant limiting situations can be discussed. Given ψ, if τ_M is such that the key length parameter $(6\,K\,\tau_M)^{1/2}$ is smaller than the typical thickness of the Galactic disk, h, the result will be equivalent to that of a uniform density in a three dimensional volume, hence

$$C_{3D}(\psi) = \int_\psi^\infty p(\psi')\,\mathrm{d}\psi' = \int_0^{\tau_M} \mathrm{d}t\,\frac{4}{3}\pi d^3\,\rho(\boldsymbol{r}, t)\Big|_{d^2\,=\,-6K\tau_M x\ln(x)} = \underbrace{\frac{1}{\pi^{1/3}}\,\frac{3^{3/2}}{2^{1/3}\,5^{5/2}}\,\frac{1}{N}\,\frac{R^{4/3}\,K^{2/3}}{h\,L^{5/3}\,\nu^{2/3}}\langle\Psi\rangle^{5/3}}_{\eta_{3D}}\ \psi^{-5/3} \propto \psi^{-5/3}\ . \tag{20}$$

Notice that the coefficient η depends on the space-time probability density to find a source lying in the neighbourhood of the observer. So does the typical flux spread σ_N. We may nevertheless express it as a function of the average flux $\langle\Psi\rangle$ to exhibit how the various CR parameters at stake come into play. For the sake of clarity, the value of $\langle\Psi\rangle$ has been derived here assuming that the Galactic disk is an infinitely thin slab. Taking the 2D model neglecting radial boundary conditions leads to the simple expression

$$\langle\Psi\rangle = \frac{h\,L}{K} Q = \frac{q\,\nu\,L}{2\,\pi\,R^2\,K}\ , \tag{21}$$

whose numerical value is very close to the actual result, as shown in the Appendix. Qualitatively, we expect that the behaviour outlined in Eq. (20) is always attained for sufficiently high fluxes, since those require very close sources, although when is this regime attained depends on the energy E via the diffusion coefficient K. Lower fluxes, however, are yielded also by sources located "far away" from us, with respect to the scale h. In the limit where these dominate, one can effectively model the Galaxy as an infinitely thin disk, so that the only quantity that matters is the 2D (surface) density $\mu(\boldsymbol{r}, t)$ which may be expressed as

$$\mu(\boldsymbol{r}, t) = \frac{\nu}{\pi R^2}\frac{1}{N}\ . \tag{22}$$

In this 2D limit, one gets:

$$C_{2D}(\psi) = \int_0^{\tau_M} \mathrm{d}t\,\pi d^2\,\mu(\boldsymbol{r}, t)\Big|_{d^2\,=\,-6K\tau_M x\ln(x)} = \underbrace{\frac{3}{2^{11/3}\pi^{2/3}}\,\frac{1}{N}\,\frac{K^{1/3}\,R^{2/3}}{\nu^{1/3}\,L^{4/3}}\,\langle\Psi\rangle^{4/3}}_{\eta_{2D}}\ \psi^{-4/3} \propto \psi^{-4/3}\ . \tag{23}$$

We will argue in the following that, depending on the regime of fluxes Ψ in which one is interested, either the 2D or the 3D distribution is the relevant one to the description of the problem. In any case, by virtue of the generalized version of the central limit theorem of Sec. 3.1, we know how to derive the pdf $P(\Psi)$ for both cases. Suffice it to take an index $\alpha = 5/3$ (3D) or $\alpha = 4/3$ (2D) and to compute the spread σ_N from Eq. (16) via the corresponding coefficients η_{3D} and η_{2D}. Notice that σ_N can be expressed as a function of the average flux $\langle\Psi\rangle$ and the various CR parameters. The number of sources N has cancelled out in the product $\eta\,N$. When it is large enough, the asymptotic regime where the central limit theorem holds is reached and we expect

$$P(\Psi) \to\ \frac{1}{\sigma_N}\,S[\alpha, 1, 1, 0; 1]\left(\frac{\Psi - \langle\Psi\rangle}{\sigma_N}\right)\ . \tag{24}$$

In order to comment upon the dependencies of the spread σ_N on the parameters of the problem, one may write

$$\frac{\sigma_N}{\langle\Psi\rangle}\ \propto\ \begin{cases} \dfrac{K^{2/5}\,R^{4/5}}{\nu^{2/5}\,h^{3/5}\,L} & \text{in the 3D case,} \\ \dfrac{K^{1/4}\,R^{1/2}}{\nu^{1/4}\,L} & \text{in the 2D case.} \end{cases} \tag{25}$$

As already noticed, the number N of sources has disappeared from the rescaled quantity $\sigma_N/\langle\Psi\rangle$. The latter encodes the statistical excursions of the total flux Ψ around its mean value $\langle\Psi\rangle$. Rescaled to the mean flux, the spread has the same dependence on the height L of the diffusive halo ($\propto 1/L$) in both the 2D and 3D regimes. The thickness h of the Galactic disk only enters in the expression of η_{3D}. The relative spread $\sigma_N/\langle\Psi\rangle$ increases with CR energy through the diffusion coefficient K. It decreases as the rate ν of explosions is increased. Both K and ν enter through the ratio K/ν, with an exponent of 2/5 (3D) or 1/4 (2D).

3.3. The case with an upper cut on the flux

Strictly speaking, applying the generalized version of the central limit theorem requires that the cumulative distribution function $C(\psi)$ for a single source has a heavy-tail behaviour up to an infinite flux ψ. This behaviour should nevertheless break down since, for instance, infinite fluxes are unphysical. However, one expects physically that the stable law expression (24) for $P(\Psi)$ still provides a good approximation to the actual distribution up to some value of the total flux Ψ, should the underlying power-law behaviour of the single source pdf $p(\psi)$ be valid over a sufficiently large range. To quantify this, let us proceed with the following heuristic argument. Assume that the single source pdf follows the power-law behaviour $p(\psi) \propto \psi^{-\alpha-1}$, with $1 < \alpha < 2$, up to some critical value ψ_{cut} above which it vanishes. There may be several reasons for that, some to be explored in the following. Schematically, one can write the probability of measuring a flux ψ from a single source as:

$$p(\psi) = (1 + \epsilon)\ p_{th}(\psi)\ \Theta(\psi_{cut} - \psi)\ , \tag{26}$$

where $p_{th}(\psi)$ is the idealized pdf with an infinite power-law tail which we have discussed in section 3.1. Of course this may be a too crude approximation close to ψ_{cut}, but provided that ψ_{cut} is large compared to the fluxes of interest and the renormalization correction ϵ is small, it should not really matter. In fact, given the Ansatz of Eq. (26), one can write the probability to measure a flux $\Psi = \sum_i^N \psi_i$ from N sources, among which N are located inside the light cone, as

$$P(\Psi) = \int_{\psi_1}\int_{\psi_2} .. \int_{\psi_N} p(\psi_1)\ p(\psi_2)..p(\psi_N)\ \delta\left(\sum_i^N \psi_i - \Psi\right)\ \mathrm{d}\psi_1\mathrm{d}\psi_2..\mathrm{d}\psi_N\ , \tag{27}$$

$$= (1 + \epsilon)^N \int_{\psi_1} .. \int_{\psi_N} p_{th}(\psi_1)..p_{th}(\psi_N)\ \Theta(\psi_{cut} - \psi_1)..\Theta(\psi_{cut} - \psi_N)\ \delta\left(\sum_i^N \psi_i - \Psi\right)\ \mathrm{d}\psi_1..\mathrm{d}\psi_N\ . \tag{28}$$

For values of Ψ such as $\Psi < \psi_{cut}$[2], each individual value ψ_i must satisfy $\psi_i < \psi_{cut}$. Hence we get

$$P(\Psi) = (1+\epsilon)^N \int_{\psi_1} .. \int_{\psi_N} p_{th}(\psi_1)..p_{th}(\psi_N)\, \delta\left(\sum_i^N \psi_i - \Psi\right) \mathrm{d}\psi_1..\mathrm{d}\psi_N \;\text{ for }\; \Psi < \psi_{cut}\ . \tag{29}$$

Thus, for N *sufficiently* large, we expect

$$P(\Psi) \approx (1+\epsilon)^N \frac{1}{\sigma_N}\, S[\alpha,1,1,0;1]\left(\frac{\Psi - \langle\Psi\rangle_{th}}{\sigma_N}\right) \quad \text{for} \quad \Psi < \psi_{cut}\ (\star)\,, \tag{30}$$

where the average flux $\langle\Psi\rangle_{th}$ in the argument of the stable function corresponds to the uncut idealized pdf $p_{th}(\psi)$. The approximation of Eq. (30) is quite general, but its actual usefulness depends on the precise values of ψ_{cut} and ϵ. For instance, as long as $N\epsilon \ll 1$, the result does not really depend on ϵ. That condition turns out to be satisfied for the cases which are subsequently discussed. In the following subsections, we actually distinguish two evident physical reasons that impose a cut on the tail of the pdf distribution.

3.4. Causality effect

To commence, propagation through diffusion should not violate causality, a condition which is not always satisfied by the propagator as defined in Eq. (3). Taking any finite age τ for a source leads to a non-zero value for $\mathcal{G}$, whatever the distance d. This will not cause much trouble for far and young sources for which the flux is exponentially suppressed, but for young and close objects, which happen to dominate large positive fluctuations of Ψ with respect to the average value $\langle\Psi\rangle$, this can lead to much larger flux contributions than physically allowed.

A correction for this effect can be quantified with reference to the space-time diagram of Fig. 1 by removing, from the region of phase space that contributes to the flux, the portion where causality is violated. The domain to be withdrawn extends above the orange curve defined by the light cone condition $d^2 = c^2x^2\tau_M^2$, c being here the speed of light. The orange parabola allows to carve away the domain in white that lies below the blue line, leaving only the light-blue shaded region to contribute to fluxes larger than ψ. The intersection between the blue (diffusion) and orange (light cone) curves takes place at $x = x_0$ for which

$$-\beta\, x_0 = \ln(x_0) \quad \text{with} \quad \beta = \frac{c^2\,\tau_M}{6K}\ . \tag{31}$$

The cumulative distribution function $C(\psi)$ has to be recalculated. It is given now by two different contributions corresponding to the integrals of the light-blue shaded area extending to the left (C_1) and to the right (C_2) of the vertical line at x_0 in Fig. 1. The 2D and 3D results may be expressed as:

$$C_{2D}^{causal}(\psi) = \pi\,\mu_{(\boldsymbol{r},t)}\, 6K \left(\frac{a}{\psi}\right)^{4/3} \left\{\left(\frac{1-x_0^2}{4}\right) + \frac{x_0^2}{2}\ln x_0\right\} + \pi\,\mu_{(\boldsymbol{r},t)}\, c^2 \left(\frac{a}{\psi}\right)^2 \frac{x_0^3}{3} \equiv C_1^{2D}(\psi) + C_2^{2D}(\psi)\,, \tag{32}$$

$$C_{3D}^{causal}(\psi) = \frac{4}{3}\pi\,\rho_{(\boldsymbol{r},t)}\,(6K)^{3/2} \left(\frac{a}{\psi}\right)^{5/3} \int_{x_0}^1 \{-x\ln(x)\}^{3/2}\mathrm{d}x + \frac{4}{3}\pi\,\rho_{(\boldsymbol{r},t)}\, c^3 \left(\frac{a}{\psi}\right)^{8/3} \frac{x_0^4}{4} \equiv C_1^{3D}(\psi) + C_2^{3D}(\psi)\ . \tag{33}$$

The larger the flux ψ, the smaller the maximal age τ_M. In this limit, the coefficient $\beta \propto \tau_M$ vanishes. As the orange parabola of Fig. 1 opens, the value of x_0 tends to 1 and a large fraction of the space-time volume becomes causally disconnected. Thus, in the high flux limit, C_1 vanishes while C_2 increases. In the 2D regime, $C_{2D}(\psi) \propto \psi^{-2}$ whereas in the 3D regime, $C_{3D}(\psi) \propto \psi^{-8/3}$. As mentioned previously, the latter eventually takes over the former for very large values of the flux ψ for which the typical distances of the sources are smaller than the thickness h of the Galactic disk. As $8/3 > 2$, the variance associated to the pdf $p(\psi)$ is now finite. According to the central limit theorem, the probability $P(\Psi)$ converges toward a Gaussian when the number of sources N goes to infinity. Notice incidentally that if the Galactic disk was infinitely thin, with $h = 0$, the 2D regime would apply with $\alpha = 2$. The variance is in that case divergent but the generalized central limit theorem can be applied, with the consequence that the total flux pdf $P(\Psi)$ reaches a Gaussian form too. Although *per se* causality arguments would allow arbitrarily large fluxes, we see that the whole discussion on stable laws loses its importance once a sizable fraction of the space-time volume is removed, since $p(\psi)$ is too steep. In practice, one can account for these effects by abruptly cutting the "standard" power-law distribution pdf above a transition flux $\psi_{cut} \equiv \psi_c$, which we may define for instance via the condition $C_1(\psi_c) = C_2(\psi_c)$. As we are interested in computing probabilities around the mean value $\langle\Psi\rangle$, let us compute ψ_c and compare it with $\langle\Psi\rangle$. To do so, we need to determine (ψ_c, x_c) by solving the two following equations:

$$C_1(\psi_c) = C_2(\psi_c) \text{ and } -\beta_c(\psi_c)\, x_c = \ln(x_c)\,, \tag{34}$$

which numerically yields $x_c \approx 0.6226$ in the 2D case and $x_c \approx 0.6424$ in the 3D case. Note that x_c (or equivalently β_c) does not depend on the cosmic ray energy, and is not very different between the 2D and 3D regimes. We can also define $y = \psi_c/\langle\Psi\rangle$, which can be written as

$$y = \frac{\psi_c}{\langle\Psi\rangle} = \frac{1}{4\,6^{3/2}\sqrt{\pi}}\,\frac{1}{\beta_c^{3/2}}\,\frac{c^3\,R^2}{K^2\,L\,\nu}\ . \tag{35}$$

[2] This condition is denoted hereafter by a ($\star$)

The estimate for y varies only by 14% between the 2D and 3D cases. As this difference is quite small, we will take the average between these two values in the following discussion. Notice that y depends on energy through the diffusion coefficient K. Of course, for our discussion to be of any relevance, the stable law Eq. (30) should be valid for a total flux Ψ well in excess of its average $\langle\Psi\rangle$, i.e., for values of y as large as possible. As an example, for the MED propagation model borrowed from Donato et al. 2004, we find that $y \simeq 32$ at 10 TeV while it reaches $\sim 2 \times 10^4$ at 100 GeV.

The evolution of $\psi_c/\langle\Psi\rangle$ as a function of energy is displayed in grey in Fig. 2 for the three different benchmark propagation models discussed in Donato et al. 2004, namely MIN, MED and MAX. That ratio is always larger than 10 for cosmic ray energies below 10 TeV. To be conservative, the causality constraint could be forgotten below the TeV scale as long as we are interested in values of Ψ not exceeding a few times the average. However, depending on the propagation model, the light cone cut-off may seriously impair the use of Eq. (30) above a few tens of TeV, an energy range probed by calorimetric instruments such as CREAM or CALET.

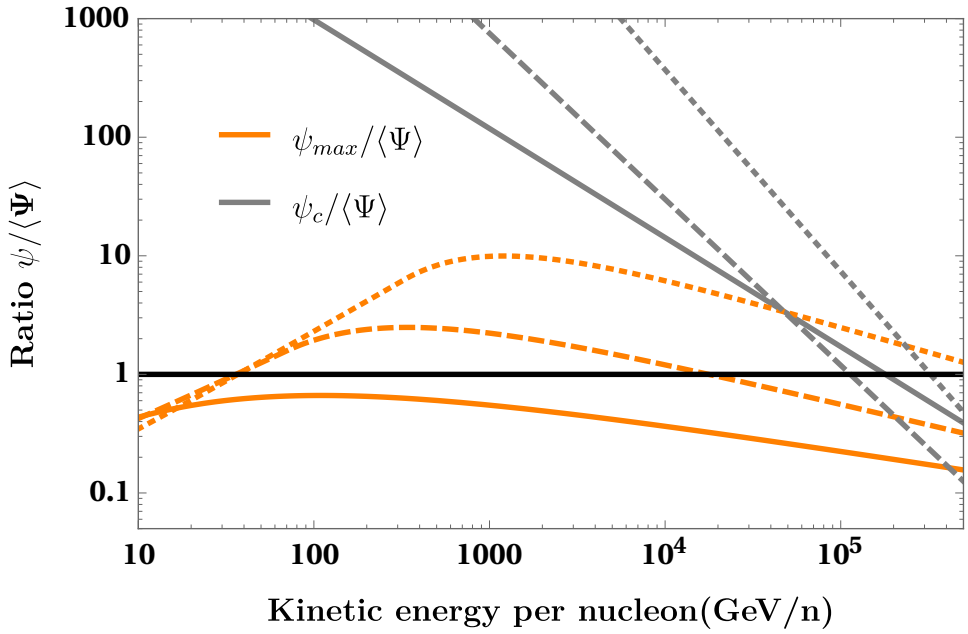

Fig. 2. The causal cutoff flux $\psi_c/\langle\Psi\rangle$ (local environment cutoff flux $\psi_{max}/\langle\Psi\rangle$) as a function of energy is displayed in grey (orange) from top to bottom for the three propagation models MIN (dotted), MED (dashed) and MAX (solid).

3.5. Absence of very close and/or young sources

Another natural limitation to the maximum flux that a single source may contribute to the measured CR flux Ψ comes from some (partial) deterministic information on nearby sources. In a schematic way, one may split the flux as the sum of a local contribution, from known sources, and a remote component, on which the only information is of statistical nature, as considered above[3]:

$$\Psi = \Psi_{\rm loc} + \Psi_{\rm far} \ . \tag{36}$$

For a given catalogue, which is assumed to be complete within a given region of space-time, from which the contribution $\Psi_{\rm loc}$ can be "exactly" computed, one could repeat the reasoning of the previous section to determine the pdf associated to $\Psi_{\rm far}$. The cumulative distribution function $C(\psi)$ of a remote source can be computed by carving out the space-time region covered by the catalogue.

Let us develop instead a slightly simpler argument by determining the maximal flux $\psi_{cut} \equiv \psi_{max}$ one can expect from a source located at the inner boundary of the phase space region filled by the catalogue. We can use it to find the closest and youngest object, hence deriving plausible values for the minimal distance and age below which no cosmic ray injection takes place. A source located at distance d and which exploded a time τ in the past contributes the flux

$$\psi \ = \ \frac{q}{(4\,\pi\,K\,\tau)^{3/2}}\,\exp\left(-\frac{d^2}{4K\tau}\right) . \tag{37}$$

In the most general case, we want to put lower limits on the distance ($d > d_c$) and age ($\tau > \tau_c$) of remote sources in order to extract the cut-off, hereafter denoted by ψ_{max}, above which the pdf $p(\psi)$ vanishes. Constraining the distance d to be larger than d_c translates into the maximal flux

$$\psi_M = \frac{q}{(2\,\pi\,d_c^2/3)^{3/2}}\,\exp\left(-\frac{3}{2}\right) , \tag{38}$$

[3] The situation may be intermediate, for instance one has a catalogue whose completeness decreases with distance and age of the source, but accounting for this complication is unnecessary for what follows.

which is reached for an age $\tau_{max} = d_c^2/6K$. The flux ψ_M corresponds to the solid grey curve of Fig. 3. In this space-time diagram, the region below $d = d_c$ is excluded. From now on, two cases must be distinguished depending on the relative values of τ_{max} and τ_c. If $\tau_{max} > \tau_c$, the maximum flux which a remote source may provide is still ψ_M, a value reached at the space-time location (τ_{max}, d_c). On the other hand, if $\tau_{max} < \tau_c$, the region to the left of the vertical line $\tau = \tau_c$ being excluded, remote sources can no longer yield the flux ψ_M. The solid grey line lies entirely in the excluded portion of the phase space diagram of Fig. 3. In this regime, the maximal flux attainable by a remote source is $\psi'_M < \psi_M$. It corresponds to the dashed grey line which touches the allowed phase space region at location (τ_c, d_c).

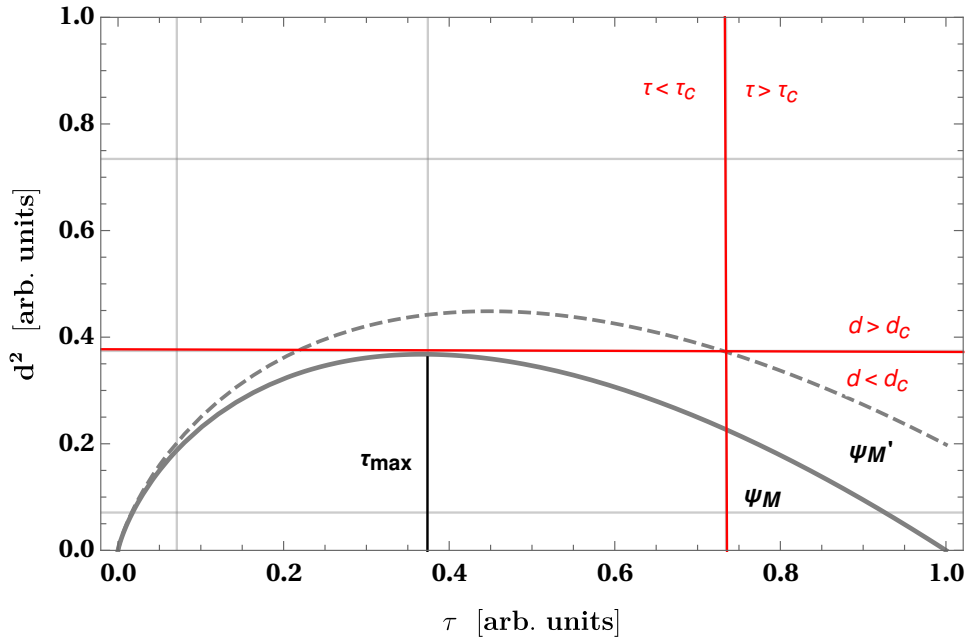

Fig. 3. Solid grey line: locus of source ages and distances giving the same flux as the maximal one ψ_M yielded by a source located at distance d_c from the Earth, attained for $\tau = \tau_{max} = d_c^2/6K$. Dashed grey line: locus of source ages and distances giving the same flux ψ'_M as the one of a source of age τ_c and distance d_c. In the case shown ($\tau_{max} < \tau_c$) the flux ψ'_M is also the maximal flux a source farther than d_c and older than τ_c.

In summary, imposing the constraint $\{d > d_c,\ \tau > \tau_c\}$ translates into $\psi < \psi_{max}$ with:

$$\psi_{max} = \begin{cases} \psi_M \equiv \dfrac{q}{(2\pi d_c^2/3)^{3/2}} \exp\left(-\dfrac{3}{2}\right), & \text{if } \tau_{max} \equiv d_c^2/6K > \tau_c\ , \\ \psi'_M \equiv \dfrac{q}{(4\pi K \tau_c)^{3/2}} \exp\left(-\dfrac{d_c^2}{4K\tau_c}\right), & \text{if } \tau_{max} < \tau_c\ . \end{cases} \tag{39}$$

This value may be compared to the mean flux $\langle\Psi\rangle$ taken as the theoretical average corresponding to the slab model and derived in Annexe. A. The relations (39) readily translate into

$$\frac{\psi_{max}}{\langle\Psi\rangle} = \begin{cases} \dfrac{3R^2K}{\nu L d_c^3}\sqrt{\dfrac{3}{2\pi}} \exp\left(-\dfrac{3}{2}\right), & \text{if } \tau_{max} > \tau_c\ , \\ \dfrac{R^2}{4\nu L\sqrt{\pi K \tau_c^3}} \exp\left(-\dfrac{d_c^2}{4K\tau_c}\right), & \text{if } \tau_{max} < \tau_c\ . \end{cases} \tag{40}$$

As a conservative example of this procedure, we have taken $d_c = 0.06$ kpc as our lower limit on the distance, inspired by the closest known source G+276.5+19. In the same way, our lower bound on the age comes from the youngest known source J0855-4644 for which $\tau_c = 2.7$ kyr. These values are taken from the catalogue compiled by Delahaye et al. (2010). Using relations (40), we have derived the ratio $\psi_{max}/\langle\Psi\rangle$ and plotted it in orange in Fig. 2 to compare it with $\psi_c/\langle\Psi\rangle$. We observe a change of slope in the dependence of $\psi_{max}/\langle\Psi\rangle$ as a function of cosmic ray energy. This is particularly obvious in the MIN case (dotted orange curve) for which the diffusion coefficient is the smallest at low energies compared to the other propagation regimes MED and MAX. In the MIN configuration, the ratio $\psi_{max}/\langle\Psi\rangle$ increases with energy below 1 TeV. In this regime, K is small and the critical age $\tau_{max} = d_c^2/6K$ exceeds the lower bound τ_c. According to Eq. (40), the ratio $\psi_{max}/\langle\Psi\rangle$ scales as K and increases with cosmic ray energy. At approximately 1 TeV, a change of regime occurs when τ_{max} becomes smaller than τ_c, and the ratio $\psi_{max}/\langle\Psi\rangle$ scales as $1/\sqrt{K}$, decreasing with energy. The same trend is featured by the MED (dashed orange) and MAX (solid orange) curves, although in a milder way.

As clearly shown in Fig. 2, the cut-off ψ_{max} imposed by the catalogue of local and recent sources is much more constraining than the value ψ_c yielded by the causality argument. The orange curves are basically always below the grey lines, which they intersect at energies in excess of 200 TeV, and for values of the ratio $\psi_{cut}/\langle\Psi\rangle$ of order 1. The use of approximation (30) is therefore possible below the orange curves. It is effectively interesting for values of the cut-off ψ_{max} larger than the average flux $\langle\Psi\rangle$. This is not the case of the MAX configuration. For the MIN and MED propagation models, the stable law (30) can still be applied on a fairly limited region in energy and total flux Ψ. As featured in Fig. 2, the ratio $\psi_{max}/\langle\Psi\rangle$ reaches a maximal value of 10 at an energy of 1 TeV. The constraint from the catalogue is therefore quite strict. Most of the populations of sources which would otherwise lead to large values of the cosmic ray flux are excluded from the statistical analysis when the age and distance constraints are imposed. A word of caution is in order though, since the completeness of a catalogue is always questionable. Setting lower limits on the age and distance of nearby sources may be quite subjective and eventually hazardous. That is why we have disregarded them in the Monte Carlo simulations which we discuss in the next section.

4. Comparison with numerical simulations

Till now, we have determined for a given propagation setup the range of fluxes Ψ over which the approximation described in Sect. 3.3 holds. However, just like the combined pdf $P(\Psi)$ tends toward a Gaussian law when the conventional central limit theorem applies, the convergence to a stable law is only an asymptotic behaviour. While exact results on the closeness to a stable law at finite N may exist in the mathematical literature, generic results are not useful in our case where a cut-off may be imposed on the individual flux pdf $p(\psi)$. We thus need to validate the reliability of the analytical theory via extensive numerical simulations. Our aim is to study how the total flux pdf $P(\Psi)$ converges to or departs from the stable law Eq. (24).

For each realization of Ψ, we simulate a Galactic population of sources in the framework of the 3D model of Eq. (6). Each source is generated at the random position $\mathbf{x_i}$ within the Galactic disk, and with the random age τ_i. The positions $\mathbf{x_i}$ are taken within an idealized cylindrical Milky Way Galaxy of radius R and half-thickness h, so that the spatial density of sources is homogeneous within the disk. The age of each source τ_i is taken between 0 and T, where T is the integration time of the simulation and is chosen to be $3\ \pi L^2/4\ K$, i.e., roughly three times the typical diffusion time within the magnetic halo. The number of sources of a realization is $N = T\nu$, with ν the rate of SN explosions, taken here to be 3 per century [4]. In our model, this number reaches about 4×10^6 at a reference energy of 100 GeV. The spectrum of particles injected by each source is defined as

$$q = q_0 \left(\frac{\mathcal{R}}{1\,\mathrm{GV}}\right)^{-2.2}\ , \tag{41}$$

where $\mathcal{R}$ stands for the CR rigidity while the normalization q_0 is set equal to 1 GeV^{-1}. Notice that q does not come into play insofar as it can be factored out from our numerical results. The flux yielded by a source is computed assuming the CR propagation model MED, where we have safely neglected the effects of convection, diffusive reacceleration and spallations which become negligible at the energies considered in our simulations. Without loss of generality, fluxes are derived for an observer placed at the radial and vertical centers of the Galactic disk, i.e., at $r = z = 0$. The contributions ψ_i of the N sources of a given population are added to obtain one realization of Ψ. When the causality condition discussed in Sec. 3.4 is implemented, the contributions from sources lying outside the light cone of the observer are not included. We evaluated Ψ for each decade of energy between 100 GeV and 1 PeV. As we are interested in the pdf of the random variable Ψ, we simulated "only" 10^6 realizations of an idealized cylindrical Milky Way Galaxy, since we hardly care about probabilities below the 10^{-5} level.

In Fig. 4, we show the results of the simulations which we carried out at 100 GeV, 1 TeV and 10 TeV, with the light cone cut-off switched on. In each row, the left and right cumulative blue histograms of 10^6 realizations of Galactic populations of CR sources are respectively displayed in the left and right panels, whereas the pdf $P(\Psi)$ stands in the middle. Once normalized to unity, the cumulative histograms on the left and on the right yield directly the probability to get a population sourcing a flux respectively smaller or larger than the value $\Psi/\langle\Psi\rangle_{sim}$ read on the horizontal axis. Notice that $\langle\Psi\rangle_{sim}$ denotes the value of the flux averaged over the 10^6 realizations of our Monte Carlo. Due to finite sampling, results start to become unreliable for probabilities below 10^{-5}, and are obviously not even defined below 10^{-6}.

In each of the panels of Fig. 4, we also display the left and right cumulative distributions as well as the pdf corresponding to the theoretical predictions of Sec. 3.2. The dashed red line stands for the 3D case (i.e., $\alpha = 5/3$) whereas the solid green curve refers to the 2D case (i.e., $\alpha = 4/3$). In the argument of the stable distribution of Eq. (24), the average flux $\langle\Psi\rangle$ must be calculated exactly, assuming the same Milky Way magnetic halo as in the Monte Carlo simulations, namely a disk of radius 20 kpc and a maximal age for the SN explosions of T. Depending on whether the theoretical prediction is 2D or 3D, the sources are distributed along the vertical direction according to Eq. (6). As shown in the Appendix, the precise value of $\langle\Psi\rangle$ is slightly different from the approximation of Eq. (21). Once derived, the argument of the stable distribution (24) must be carefully rescaled to match the variable $\Psi/\langle\Psi\rangle_{sim}$ used on the horizontal axes of Fig. 4. For completeness, the residuals between the models (2D and 3D) and the histograms are also displayed below each panel. The shaded areas correspond to the one-sigma Poissonian uncertainty coming from the histogram binning. Finally, the dashed-dotted blue line depicts the results expected from a Gaussian distribution with the same average and variance as given by the simulations. That variance is finite insofar as the light cone cut-off condition is implemented.

For energies not in excess of 10 TeV, the first noticeable result is the remarkable good convergence of the simulations toward the analytical model based on stable distributions. At low fluxes, the pdf and the left cumulative distribution of the simulations are very well matched by the theoretical 2D curve, and this holds whatever the energy considered. On the other hand, the theoretical

[4] Note that for a constant explosion rate of 3 SN/century and the choosen T, this means considering only sources younger than about 133 Myr at 100 GeV, so still much younger than the age of the Galaxy.

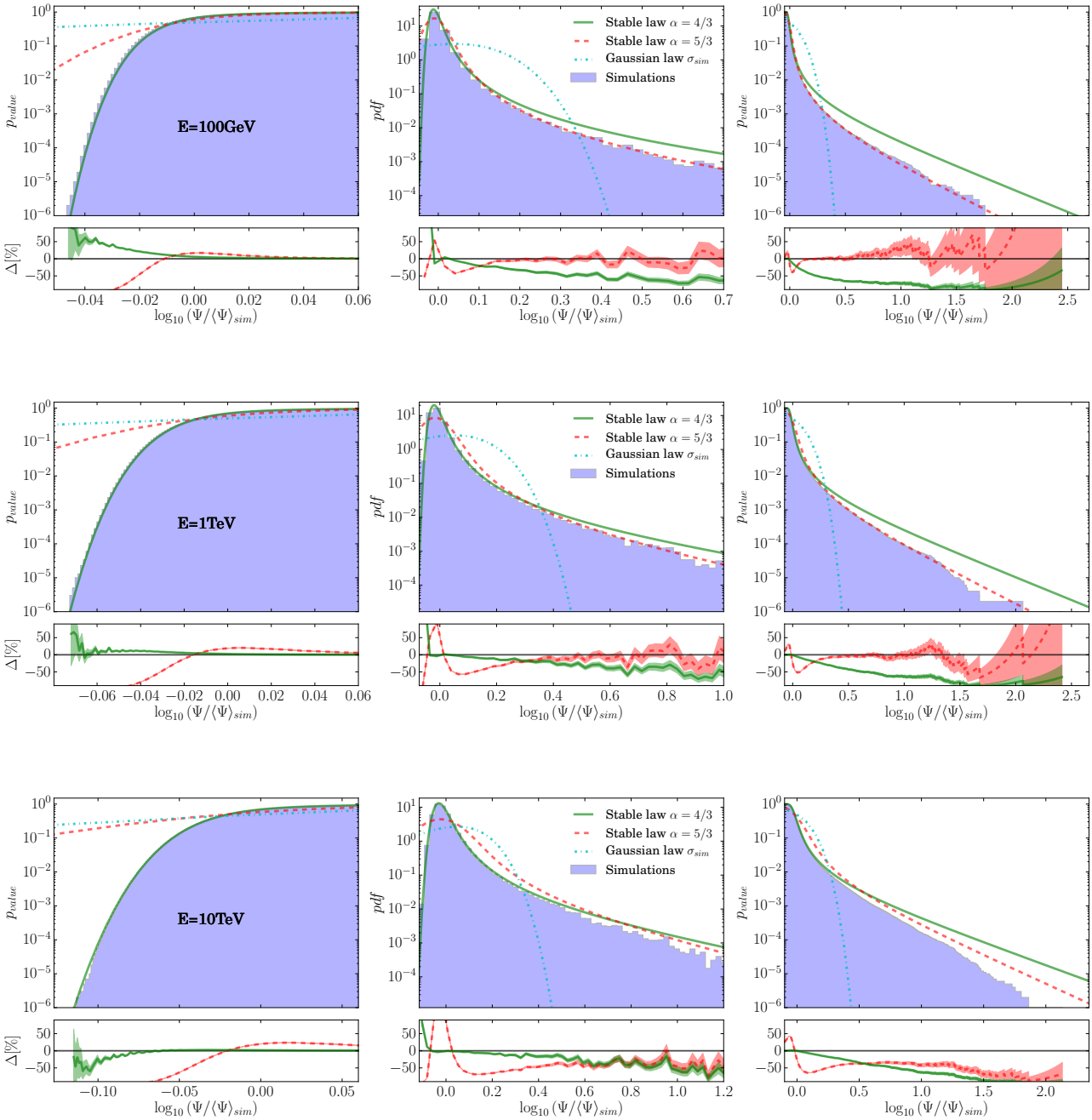

Fig. 4. For each row, the left and right cumulative blue histograms of 10^6 Monte Carlo realizations of Galactic populations of CR sources are respectively displayed in the left and right panels, whereas the pdf $P(\Psi)$ stands in the middle. The MED propagation model is used without taking into account convection, diffusive reacceleration and spallations. From top to bottom, the CR kinetic energy has been set equal to 100 GeV, 1 TeV and 10 TeV. The solid green line indicates the theoretical prediction for the 2D model of the Galactic magnetic halo, whereas the dashed red curve correponds to the 3D case. The residuals between theory and simulations are displayed below each histogram with their 1-σ Poissonian error.

prediction of the 3D model is always the closest to the simulations for large fluxes. Whatever the regime, all histograms reproduce the theoretical probability within O(10%) down to the 10^{-4} level, and even with the order of magnitude below 10^{-5}. Note that whatever the energy in the range extending from 100 GeV to 1 PeV, the simulations are not at all reproduced by the Gaussian law, featured by the dashed-dotted blue lines, which would be the limiting case for an infinite number N of sources according to the conventional central limit theorem. Stable laws are on the contrary an excellent approximation to our results, even though a cut has been imposed on the single source pdf $p(\psi)$ from causality considerations and one would naively expect $P(\Psi)$ to relax toward a Gaussian law.

At fixed CR energy, we observe a transition occuring at some critical value ψ_h of the flux Ψ, above which the 3D (i.e., $\alpha = 5/3$) stable law yields a better approximation than the 2D (i.e., $\alpha = 4/3$) distribution. In order to derive an estimate for ψ_h, we should

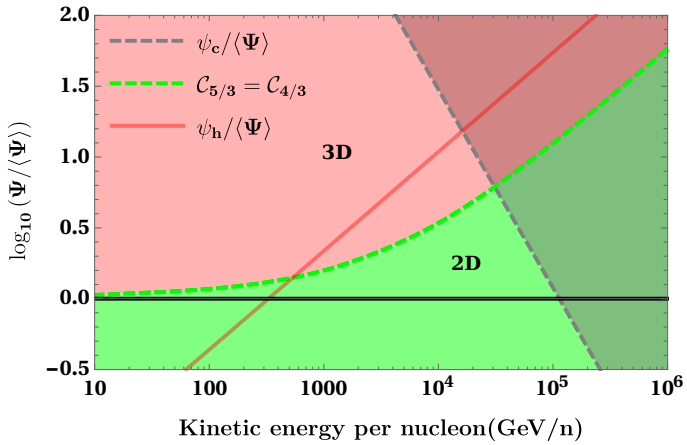

Fig. 5. Regions in the flux versus energy plane where the 2D or 3D stable law is best suited to compute the probability of an excess above the mean (MED propagation model assumed). For a fluctuation lying in the light red (green) region, one should use the 3D (2D) approximation corresponding to the index $\alpha = 5/3$ ($\alpha = 4/3$). The dashed green curve signals the transition between these regimes as estimated from the equality of the cumulative distributions, $C_{5/3} = C_{4/3}$. The solid red line reports the alternative estimate of ψ_h following the argument developed in the text. In the shaded area in the upper-right corner of the diagram, causality is expected to generate deviations from the stable law behaviour as a result of the light cone cut-off ψ_c it implies on the pdf.

keep in mind that stable laws tend to be dominated by the contribution from a single object. The transition between the 2D and 3D regimes of the total flux pdf $P(\Psi)$ should result from an evolution in the behaviour of the individual flux pdf $p(\psi)$ with respect to ψ. This change is in turn related to a modification in the spatial distribution of the sources. We remark that the closer the object, the higher the flux it yields. Let us now make an educated guess and define ψ_h as the critical flux above which the dominant sources are statistically very close to the observer, at a distance less than the half-thickness h of the Galactic disk. As seen by the observer, they are isotropically distributed and the 3D model applies. As objects yielding a flux less than ψ_h are farther, their spatial distribution reflects the flatness of the Galactic disk and the 2D model is best suited to describe the simulations. In the phase space diagram of Fig. 3, the flux ψ_h corresponds to the solid grey iso-flux curve where d_c is replaced by h. A value can be derived from Eq. (38) and translates into the red solid line of Fig. 5 that depicts the behaviour of the ratio $\psi_h/\langle\Psi\rangle$ as a function of CR kinetic energy. That curve features the same trend as our results. As the CR energy increases, the 2D to 3D transition occurs at higher values of the flux relative to the average $\langle\Psi\rangle$. At low CR energy, the agreement is not very good though. The transition flux ψ_h falls beneath the average flux for energies below 300 GeV, a trend that is not oberved in our simulations. In the upper-left panel of Fig. 4, the left cumulative histogram is very well matched by the 2D stable law. Furthermore, defining ψ_h as the maximal flux yielded by sources located at a distance d_c exactly equal to h is somewhat arbitrary.

If we are interested in quantifying the probability of measuring a particular flux excess with respect to the mean, as is the case for the applications discussed in Sec. 5, we can alternatively define ψ_h as the value for which the 2D and 3D right cumulative distributions $C(\psi)$ are equal. Following the notations of Eq. (14), the value of ψ_h is now given by the condition $C_{4/3}(\psi_h) = C_{5/3}(\psi_h)$. This leads to the dashed green line of Fig. 5 whose behaviour with respect to CR energy exhibits the same trend as the red curve of the previous estimate. This time, the transition flux is always larger than the average $\langle\Psi\rangle$. The dashed green line separates the plot in two distinct regions. In the light green domain extending below the frontier, the simulations are well explained by the theoretical 2D stable law (i.e., $\alpha = 4/3$). In the light red part of the diagram, the 3D stable distribution (i.e., $\alpha = 5/3$) provides the best approximation. Above 1 TeV, our new value of the transition flux is smaller than the previous estimate derived from the Galactic disk half-thickness argument. Indeed, the cumulative distribution $C(\psi)$ is obtained via an integration of the pdf $p(\psi)$ from ψ upward. It contains information pertaining to the high-flux behaviour of the pdf, and feels the 3D regime for smaller values of the flux compared to the other approach. Below 100 GeV, the 3D and 2D stable laws should be respectively used above and beneath the mean flux, indicated in the plot by the solid black horizontal line.

The shaded area in the upper-right corner of Fig. 5 lies above the dashed grey curve featuring the ratio $\psi_c/\langle\Psi\rangle$. In this region, causality is expected to limit the statistical excursions of the flux toward high values, and the stable law should overestimate the actual pdf $P(\Psi)$. This trend is already present in the lower-right panel of Fig. 4, where the right cumulative blue histogram lies below the dashed red curve of the 3D stable law. For the simulations performed at 100 GeV and 1 TeV, the agreement is excellent. According to Fig. 5, the light cone cut-off starts to seriously affect the (not too large) fluctuations of the flux above an energy of 10 TeV. To illustrate this effect, we show in Fig. 6 the results of simulations realized at 100 TeV, for which the causality constraint has been switched on (upper row) or off (lower row). The behaviour of the pdf $P(\Psi)$ is very different between the two cases. In the upper row, sources lying outside the light cone of the observer are removed. The discrepancy between the simulated histograms and the stable law predictions is striking, even for fluctuations only 30% larger than the mean. If now all the sources are allowed to contribute to the flux Ψ, the agreement between the histograms and the stable laws is recovered. In the lower-right panel of Fig. 6, the 2D prediction $C_{4/3}$ for the right cumulative distribution accounts well for the Monte Carlo results up to a flux ~ 10 times larger than the mean. For larger fluctuations, the 3D function $C_{5/3}$ is a good match to the histograms.

A last remark is in order. According to Fig. 5, the ratio $\psi_c/\langle\Psi\rangle$ drops below unity for energies above 100 TeV. In this energy range, we expect the effect of the causal cut to be so important that stable laws are poor representations of the actual pdf $P(\Psi)$ which they overshoot by far. As discussed above, this occurs as soon as the flux exceeds its mean value. But for values of Ψ lower than

the average $\langle\Psi\rangle$, the 2D stable law prediction (solid green curve) is still in excellent agreement with the histograms, whether the light cone cut-off condition is implemented or not. In this regime, small fluxes are involved with two consequences. Distant sources dominate the faint signal received by the observer and their spatial distribution reflects the flatness of the Galactic disk, which is 2D in nature. Moreover, they yield a flux ψ well below the light cone cut-off ψ_c to which they are totally insensitive. Notice the excellent agreement between the simulations and the 2D stable law predictions in all the left panels of Fig. 4 and 6. We must finally conclude that for fluxes smaller than the mean, the pdf $P(\Psi)$ has asymptotically relaxed toward the (2D) stable distribution of Eq. (24), even though this is not the case in the high-flux regime. Stable laws seem to be robust descriptions of the pdf $P(\Psi)$ as soon as condition of Eq. (15) is fulfilled over some range of values of ψ.

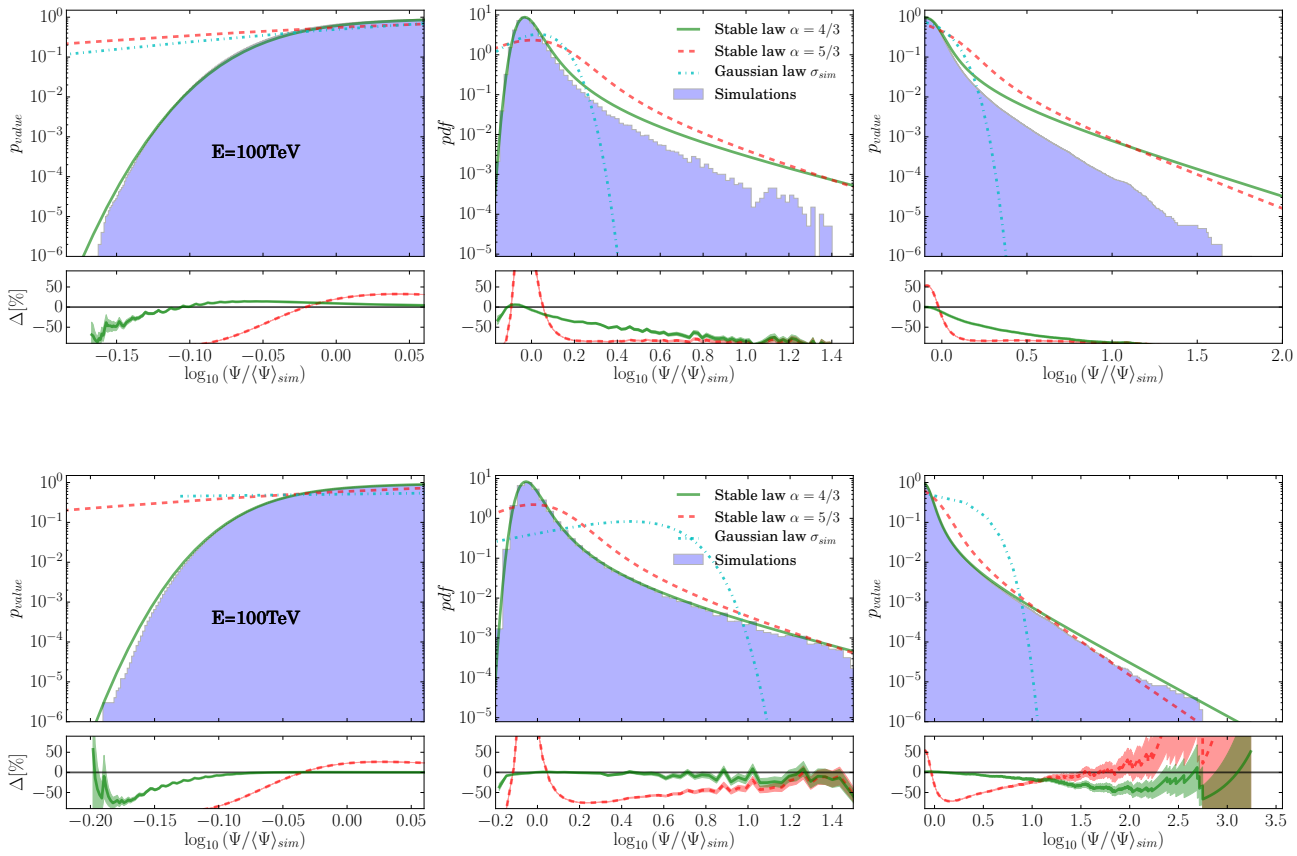

Fig. 6. Same as in Fig 4 with a CR kinetic energy of 100 TeV. The upper row features the results of a simulation where the causality constraint is implemented whereas in the lower row, all sources are taken into account in the calculation of the flux Ψ, including those lying outside the light cone of the observer.

5. Applications

In this section we present some applications of the theory developped above. At first, we want to gauge if the present precision of experimental data is sufficient to be sensitive to a fluctuation of the flux coming from the discretness of the sources. To do so we compute the probability that a source configuration leads to a 3σ fluctuation above and below the average flux assumed to follow a power law spectrum in energy. We actually calculate this probability for the proton flux measured by AMS02 and PAMELA. The results are reported Table 1 for the energies of 50 GeV an 1 TeV and for the three benchmark models MIN, MED and MAX. Each box of the table corresponds to the energy given at the top of its column. The upper value is the probability to get a fluctuation above 3σ, and the value at the bottom corresponds to the probability to have a fluctuation below 3σ. The first noticeable feature is that the probability to see a 3σ fluctuation above the mean is always different than a 3σ fluctuation below. This is a consequence of the huge asymmetry of the stable distribution. Fluctuations below the mean are strongly prevented below the brutal fallout of the pdf. Furthermore, the probability to measure a 3σ deviation from the mean is always larger at 50 GeV than at 1 TeV. This result means that the experimental uncertainty increases faster than the typical spread of the stable law with the energy. Thus, by improving data precision thanks to higher statistics or a new experiment, the probability to observe deviation from the mean flux at *low* energies ($\approx$50 GeV) increases. Regarding the different propagation models, we notice that a fluctuation in the MAX model with a large halo height is much less expected than a fluctuation for small halo models which MIN belongs. In other words, the fact that AMS02 proton data does not show any departure from a power law spectrum at relatively low energies, can be interpreted as an independent hint for large halo size models. Finally, comparing PAMELA results with AMS02, we notice that the latter has made a

Models	PAMELA		AMS02	
Model	50GeV $p\,(\Psi > \langle\Psi\rangle + 3\sigma)$ $p\,(\Psi < \langle\Psi\rangle - 3\sigma)$	1TeV $p\,(\Psi > \langle\Psi\rangle + 3\sigma)$ $p\,(\Psi < \langle\Psi\rangle - 3\sigma)$	50GeV $p\,(\Psi > \langle\Psi\rangle + 3\sigma)$ $p\,(\Psi < \langle\Psi\rangle - 3\sigma)$	1TeV $p\,(\Psi > \langle\Psi\rangle + 3\sigma)$ $p\,(\Psi < \langle\Psi\rangle - 3\sigma)$
MIN	0.15 0.13	0.083 $< 10^{-6}$	0.28 0.63	0.26 0.51
MED	0.047 $< 10^{-6}$	0.014 $< 10^{-6}$	0.16 0.26	0.12 0.0025
MAX	0.009 $< 10^{-6}$	0.0018 $< 10^{-6}$	0.045 $< 10^{-6}$	0.016 $< 10^{-6}$

Table 1. Probability that a source configuration leads to a 3σ fluctuation above and below the flux measured by AMS02 and PAMELA. The calculation is made for the three benchmark propagation models MIN, MED and MAX, and for the two energies 50 GeV and 1 TeV.

Models	MIN	MED	MAX
Probabilities(Stable law 5/3)	0.0072	0.0012	0.00016
Probabilities(Gaussian law)	0.06	10^{-5}	0

Table 2. Probabilities to obtain a flux larger than $2.86\langle\Psi\rangle$ at 1 TeV in the myriad model, calculated for three benchmark propagation models MIN, MED and MAX. The Gaussian probability is extracted from the simulation and crucially depends on the integration time of the simulation.

big step forward in reducing the experimental uncertainties, giving hopes to see deviation of the power law independently from the propagation models.

A positive large flux fluctuation corresponds to the situation where some of the sources are very near and very young. The extreme case for which a few sources (or even one source) dominate the contribution to the flux has been considered, for instance in Kachelrieß et al. (2015): the authors suggest to explain the low energy proton flux below $\sim O(10)$ TeV by involving the major contribution of a local SNR (within few hundreds of pc) which exploded about 2 Myr ago. According to Fig. 1 of this paper, this contribution would overcome the mean flux by a factor 2.86 at the energy of 10^3 GeV. In our myriad model, which assumes isotropic diffusion, the probability that a peculiar configuration of sources leads to a deviation comparable or larger to the one stated in this paper, is given by:

$$p_s = \int_{2.86\langle\Psi\rangle}^{\infty} P(\Psi)\,\mathrm{d}\Psi = 1 - \int_0^{2.86\langle\Psi\rangle} P(\Psi)\,\mathrm{d}\Psi = 1 - \underbrace{(1+\epsilon)^N}_{\approx 1 \text{ (here)}} \int_0^{\frac{2.86\langle\Psi\rangle}{\sigma_N}} S\,[\alpha, 1, 1, 0; 1](X)\,\mathrm{d}X\,. \tag{42}$$

Such a deviation corresponds to $\log_{10}(\psi/\langle\Psi\rangle) \approx 0.46$ at 10^3 GeV, for which Fig. 5 recommends the use of the 3D case corresponding to $\alpha = 5/3$. This conclusion holds for the MED model for which Fig. 5 was made, but we checked that it was actually also the case for the MIN and MAX cases. For the MIN case $\psi/\langle\Psi\rangle$ also falls below the condition $\psi_{max}/\langle\Psi\rangle$ as shown in Fig. 2.

The probabilities for the three different benchmark propagation models are reported in Tab. 2. As comparison we also display the probabilities obtained by using a Gaussian law with the variance of the simulations. In the homogeneous diffusion framework, this result suggests that the chance probability for such an excursion is at most at the level of $\sim 0.1\%$, and even one order of magnitude smaller if the MAX model, apparently closer to the recent observations, is adopted. It would not be correct to discard the model in Kachelrieß et al. (2015) based on these considerations, however, since in that article the authors advocate for a strongly anisotropic diffusion. Certainly, it emphasizes the importance of this ingredient in the plausibility of the scenario.

Another example is provided by the scenario discussed in Tomassetti & Donato (2015). Here the authors invoke a two components model for which the high energy CRs spectrum is dominated by the average Galactic population, and the low energy part by one local old source, or alternatively a population of local old sources. In this case, homogeneous diffusion is assumed. The two different energy dependences of these components would explain the break in the proton and helium flux above 200-300 GV. Once more we can compute the probability for such a low energy fluctuation of the flux in our myriad model, assuming the mean flux to be reached above the spectral break. From the Fig. 2 of this paper the proton flux at $E = 10$ GeV is dominated by some local sources which yield a value of Ψ approximately 3.3 times the average $\langle\Psi\rangle$. Within their propagation model, one can show that the probability of such an excess must be treated with the 3D case. Making use of the formula Eq. (42) of the previous example, we obtain a probability of 8.6×10^{-5}. Thus we can conclude that the only reasonable possibility for their scenario to be true is to assume a sum of two populations of sources, with the observed flux at the Earth being close to the sum of their *average* contributions rather than due to a local fluctuation.

Finally, one may consider the opposite possibility (advanced for instance in Bernard et al. 2012, 2013) for which the high-energy flux is a signature of the contribution of local sources, while the steeper flux at lower energies follows the Galactic average.

Models	MIN	MED	MAX
Probabilities(Stable law 4/3)	0.031	0.0082	0.0013

Table 3. Probabilities calculated for the most discriminating point of CREAM at 12.6TeV (the fourth one) and the three benchmark propagation models.

In Fig. 7, left panel, we display the inferred mean proton flux in the range [45-200] GeV in this model, from which data depart more and more above the energies $\gtrsim$200 GeV. To estimate the probability that such a discrepancy may occur it is crucial to check the requirement for the applicability of the stable law, i.e. $\Psi < \psi_c$. In the right panel of Fig. 7, we plot the data divided by the mean above 45 GV, together with conditions $\psi_c/\langle\Psi\rangle$ and $\psi_{max}/\langle\Psi\rangle$ of Fig. 2 (solid for MAX model, dashed for MED, dotted for MIN). If the data fall above the grey lines, it means that the observed excess cannot be provided by local sources *in the diffuse regime*. This is what happens to the two (three) highest energy CREAM data in the MED (MAX) propagation model. Strictly speaking, we can only conclude that our theory is inapplicable to those energies in the framework of these propagation models, since the diffusion approximation breaks down. However, it also means that the only way one or few local sources might account for the measured flux in that range is to assume that CR propagate quasi-ballistically from the hypothetical source(s), which would qualitatively lead to $O(1)$ anisotropy, in blatant contrast with the data, showing a dipole anisotropy in this energy range at or below the 0.1% level (see for instance the compilation in Fig. 2 of Blasi & Amato (2012)). Note also that the data fall above the orange lines, at all energies for the MAX model and already at 5 TeV for the MED one. These lines correspond to the "maximal excursion" as due to a source as young as $\tau < \tau_c = 2.7$ kyr and as close as $r < d_c = 0.06$ kpc, which is roughly the closest in space-time estimated on the basis of the available catalogue. Although the available catalogue may be incomplete, it is less and less likely so for close and young/powerful sources. This is another independent argument suggesting that a local explanation for the high-energy break of the type invoked in Bernard et al. 2012, 2013 is unlikely in propagation scenarios of the MED or MAX type. If we discard all constraints from catalogs, our theory is applicable bellow 50 TeV to estimate the probability of such an excess within our myriad model. The probability is calculated as

$$p_{value} = \int_{\Psi_{exp}}^{\infty} d\psi_{exp} \int_{0}^{+\infty} d\psi \; p(\psi_{exp}|\psi) \; p(\psi|myriad) \; , \tag{43}$$

where $p(\psi_{exp}|\psi)$ is a Gaussian law of spread σ_{exp} the experimental variance, and $p(\psi|myriad)$ is the probability to get a theoretical flux ψ in the myriad model. We compute this probability for the most constraining data point, which lies at 12.6 TeV in the CREAM data. The fluctuation at this energy is $\psi/\langle\Psi\rangle \approx 1.73$ which justifies the use of the 2D case with the stable law $\alpha = 4/3$. The results are reported Table. 3. We obtain a maximum of 3 percents within the MIN scenario. This probability is small but not vanishingly small. In fact, independent CR arguments disfavouring the MIN scenario (see for instance Lavalle et al. (2014); Giesen et al. (2015); Kappl et al. (2015); Evoli et al. (2015)) are probably even more significant in providing a killing blow to this model.

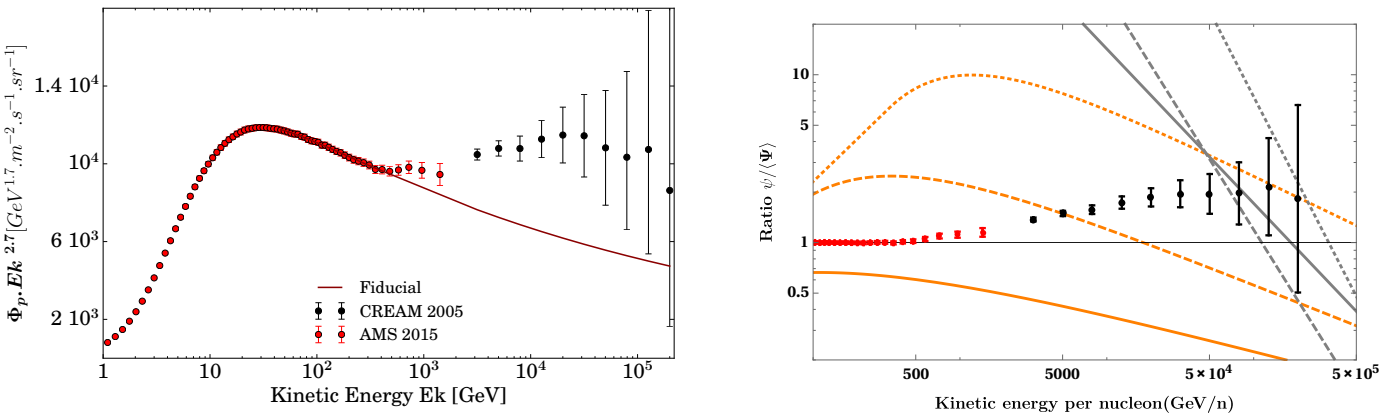

Fig. 7. Left panel: Proton flux from AMS02 (Aguilar et al. 2015) and CREAM (Yoon et al. 2011), and a fit of the spectrum between 45 GeV and 200 GeV that we assume here to be the mean Galactic flux. Right panel: data divided by the theoretical mean above 45 GeV, together with conditions $\psi_c/\langle\Psi\rangle$ and $\psi_{max}/\langle\Psi\rangle$ of Fig. 2 (solid for MAX model, dashed for MED, dotted for MIN).

6. Conclusion

Given the precision currently reached by cosmic ray measurements, it is more and more important to assess uncertainties associated to different theoretical predictions. The space-time discreteness of the cosmic ray sources is an important cause of theoretical uncertainty, given the ignorance of their precise epochs and locations, with the possible exception of the most recent and close ones.

In this article we have elaborated a statistical theory to deal with this problem, relating the composite probability $P(\Psi)$ to obtain a flux Ψ at the Earth to the single-source probability $p(\psi)$ to contribute with a flux ψ. The main difficulty arises since $p(\psi)$ is a

"heavy tail" distribution, characterized by power-law or broken power-law behaviour up to very large fluxes for which the central limit theorem does not hold, and leading to well-known *stable laws* as opposed to Gaussian distributions.

We have discussed analytically the regime of validity of the stable laws associated to the distributions arising in cosmic ray astrophysics for different propagation parameters and energy ranges, as well as the limitations to the treatment imposed by causal considerations and partial source catalogue knowledge. We have also validated our results with extensive Monte Carlo simulations.

We found that relatively simple recipes provide a remarkably satisfactory description of the probability $P(\Psi)$. We also find that a naive Gaussian fit to simulation results would underestimate the probability of very large fluxes, i.e. several times above the average, while overestimating the probability of relatively milder excursions. At large energies, large flux fluctuations are prevented by causal considerations, while at low energies a partial knowledge of the recent and nearby population of sources plays an important role.

We have applied our theory to some models recently discussed in the literature attempting to explain the spectral breaks as effects of a prominent nearby source. We showed that, at least within homogeneous and isotropic diffusion models, it is unlikely that this is the cause of the observed phenomenon, since the only case where this might happen with an appreciable probability is disfavoured by independent arguments involving secondary tracers like positrons, antiprotons, and/or the boron/carbon CR spectrum. We have also argued that the precision recently attained by cosmic ray measurements makes the observation of upwards departures from the mean expectations more likely. Actually, the close agreement of recent AMS-02 at relatively low-energies with average expectations of continuous cosmic ray source models represents by itself a constraint on propagation models, which intriguingly goes in the same direction as those recently derived from secondary species. Diffusion models with a large halo and mild energy dependence appear favoured. Another theoretically robust prediction is that no significant *downward* fluctuation with respect to average model expectations should be observed, a fact that for the time being seems confirmed by the data.

The formalism elaborated and validated in this article constitutes only a first step of a potentially much broader program. A trivial extension of the theory allows one to deal with several uncorrelated populations of sources, each one with its own distribution. A more subtle generalization would be required to deal with correlations of flux predictions at different energies. Even more challenging is to elaborate an analytical theory accounting for space and time correlations among the discrete sources of cosmic rays. Last but not least, it might be worth entertaining the possibility that some of the tools developed for applications to cosmic ray flux problems may find an application in other contexts of astroparticle physics, if not of physics in general.

Acknowledgements. We are grateful to our colleague P. Briand from the laboratory of mathematics LAMA of Université de Savoie Mont-Blanc for his kind help and for having provided us with a proof of the generalized central limit theorem.

Appendix A: What do we mean by mean

The mean flux of cosmic rays is a very useful observable whose theoretical derivation is quite simple in the high-energy limit where diffusion is the dominant propagation mechanism. Two simplifications are commonly used in the literature and lead to very good approximations compared to more sophisticated models.

To commence, sources are assumed to lie within an infinite plane with half-thickness h sandwiched by two larger diffusion volumes with height L. Inside this magnetic halo, propagation is characterised by the diffusion coefficient K. The so-called *infinite slab* model requires in addition to consider the disk as infinitely thin. In the steady state regime, the total mean flux satisfies the equation

$$-K\,\nabla^2\langle\Psi\rangle_{slab} = 2\,h\,\delta(z)\;Q\;. \tag{A.1}$$

Assuming that the CR density vanishes at the vertical boundaries $z = \pm L$, one readily gets

$$\langle\Psi\rangle_{slab} = Q\,\frac{h\,L}{K} \equiv Q\,\tau_D \quad \text{with} \quad [Q] = [\text{time}]^{-1}[\Psi]\;. \tag{A.2}$$

In this equation, Ψ is homogeneous to the density of cosmic rays expressed in particles per unit of energy and of volume or, equivalently for the discussion, to the flux expressed in particles per unit of energy, time, surface and solid angle. A simple rescaling by the factor $v_{CR}/4\pi$, where v_{CR} is the cosmic ray velocity, can be applied to switch from one quantity to the other. Choosing the former, the injection rate Q is interpreted as the number of particles injected per unit of energy, time and volume in the Galaxy. It may be useful to factorize $Q = q\,\nu/V_{\rm MW}$. Here, the spectrum q of the particles injected by a single source is expressed in particles per unit of energy. Sources appear with a rate ν. Assuming these are supernova remnants implies a value of 3 SN explosions per century. Finally, the Galactic disk with half-thickness h and radius R encompasses a volume $V_{\rm MW} = 2\,\pi\,h\,R^2$.

To go a step forward, we may now assume that the sources are no longer pinched inside an infinitely thin Galactic disk, but are spread over a vertical distance of $2h$. As long as steady state holds, the total mean flux satisfies now the equation

$$-K\,\nabla^2\langle\Psi\rangle_{vol} = \;\Theta(h - |z|)\;Q\;, \tag{A.3}$$

whose solution, derived with the same vertical boundary conditions as previously, may be expressed as

$$\langle\Psi\rangle_{vol} = \langle\Psi\rangle_{slab}\,\left(1 - \frac{h}{2\,L}\right)\;. \tag{A.4}$$

Sources extend now along the vertical direction and are no longer packed at $z = 0$. They yield a flux $\langle\Psi\rangle_{vol}$ slightly smaller than $\langle\Psi\rangle_{slab}$.

Ek (GeV)	$\langle\Psi\rangle_{slab} \equiv \langle\Psi\rangle_{2D,\ R=\infty,\ T=\infty}$	$\langle\Psi\rangle_{2D,\ R,\ T=3\tau_0}$	$\langle\Psi\rangle_{vol} \equiv \langle\Psi\rangle_{3D,\ R=\infty,\ T=\infty}$	$\langle\Psi\rangle_{3D,\ R,\ T=3\tau_0}$	$\langle\Psi\rangle_{sim}$	$\langle\Psi\rangle_{sim}^{NC}$
10^2	1.605e-01	1.599e-01	1.585e-01	1.579e-01	1.580e-01	1.579e-01
10^3	2.070e-04	2.062e-04	2.044e-04	2.037e-04	2.036e-04	2.037e-04
10^4	2.612e-07	2.601e-07	2.579e-07	2.571e-07	2.554e-07	2.577e-07
10^5	3.289e-10	3.270e-10	3.248e-10	3.236e-10	3.075e-10	3.241e-10
10^6	4.141e-13	4.105e-13	4.089e-13	4.072e-13	2.923e-13	4.071e-13

Table A.1. In this table we report the theoretical average of the flux calculated within the slab model $\langle\Psi\rangle_{slab}$, the slab model taking into account the thickness of the sources disk $\langle\Psi\rangle_{vol}$, the 2D model in the conditions of the simulations $\langle\Psi\rangle_{2D,\ R,\ T=3\tau_0}$, and the 3D model in the conditions of the simulations $\langle\Psi\rangle_{3D,\ R,\ T=3\tau_0}$. We also show the average of the flux obtained from the simulations without the contribution of non-causal sources $\langle\Psi\rangle_{sim}$, and with their contributions $\langle\Psi\rangle_{sim}^{NC}$. The values are given in units of $[\mathrm{q_0.kpc^{-2}.str^{-1}}]$ for the kinetic energies probed by the simulations.

The theoretical expression of the probability $P(\Psi)$ is provided by the stable law of Eq. (24). Its argument depends on the average value $\langle\Psi\rangle_{th}$ which should be consistently derived within the Milky Way model to which the pdf $P(\Psi)$ is associated. Although expressions (A.2) and (A.4) are excellent approximations to the theoretical mean $\langle\Psi\rangle_{th}$, they should not be used. In particular, the solid green (2D) and dashed red (3D) curves of Fig. 4 and 6 are based on the assumption that the Galactic disk has radius R and that sources cannot be older than $T = 3\tau_0$. Furthermore, all sources contribute to the theoretical average $\langle\Psi\rangle_{th}$, including those lying outside the light cone of the observer. Causality is not implemented and the heavy tail behaviour, which the theoretical pdf $p(\psi)$ should exhibit, is not suppressed.

In order to compare the theoretical pdf $P(\Psi)$ with the simulations, $\langle\Psi\rangle_{th}$ needs to be calculated from the convolution of the source term $Q(\mathbf{x}_S, t_S)$ with the diffusive propagator $\mathcal{G}_B$ over the volume of space-time $\mathcal{V}$ covered by the simulation

$$\mathcal{V} = V_{\mathrm{MW}} \times 3\tau_0 \quad \text{where} \quad \tau_0 \equiv \frac{\pi}{4}\frac{L^2}{K}\ . \tag{A.5}$$

The theoretical average corresponding to the 2D case, where the sources are pinched inside an infinitely thin disk, is denoted by $\langle\Psi\rangle_{2D,\ R,\ T=3\tau_0}$ whereas the result corresponding to the 3D case, for which the sources are vertically spread over a distance $2h$, is denoted $\langle\Psi\rangle_{3D,\ R,\ T=3\tau_0}$. These quantities are calculated as follows

$$\left.\begin{matrix}\langle\Psi\rangle_{3D,\ R,\ T=3\tau_0}\\ \langle\Psi\rangle_{2D,\ R,\ T=3\tau_0}\end{matrix}\right\} = \frac{q\,\nu}{V_{\mathrm{MW}}} \times \int_0^{3\tau_0} d\tau_S \int_0^R 2\,\pi\, r_S\, dr_S \left\{\frac{\exp\left(-r_S^2/4K\tau_S\right)}{4\,\pi\,K\,\tau_S}\right\} \int_{-h}^{h} dz_S\ \mathcal{V}_B(z_S,\tau_S) \times \begin{cases} 1 & \text{in 3D, or} \\ 2h\,\delta(z_S) & \text{in 2D.}\end{cases} \tag{A.6}$$

The function $\mathcal{V}_B(z_S, \tau_S)$ describes the CR vertical propagation and takes into account the boundary conditions at $z = \pm L$. It gauges the contribution at the observer located at $z = 0$ from a source that exploded a time τ_S ago at $z = z_S$. It can be expressed as the series

$$\mathcal{V}_B(z_S,\tau_S) = \sum_{n=-\infty}^{+\infty} (-1)^n\ \frac{\exp\left(-z_n^2/4K\tau_S\right)}{\sqrt{4\,\pi\,K\,\tau_S}} \quad \text{where the nth image is located at} \quad z_n = 2\,L\,n\ + (-1)^n\, z_S\ . \tag{A.7}$$

We notice that to recover the average of the slab model, the integral for the 2D case needs to be extended to an infinite age T and Galactic radius R. Hence we may write $\langle\Psi\rangle_{slab} \equiv \langle\Psi\rangle_{2D,\ R=\infty,\ T=\infty}$. When the same integration limits are taken for the 3D case, we recover the expression of $\langle\Psi\rangle_{vol}$, which may also be defined as $\langle\Psi\rangle_{3D,\ R=\infty,\ T=\infty}$.

In Tab. A.1, we report the average fluxes calculated with the aproaches discussed above, and compare them with the simulations. Below 10 TeV, all the values are very close to each other within $O(1\%)$. Above that energy, the mean from the simulations $\langle\Psi\rangle_{sim}$ becomes significantly lower than the theoretical one when the light cone cut-off is imposed on simulations. This effect can be checked by calculating the average flux $\langle\Psi\rangle_{sim}^{NC}$ yielded by numerical simulations for which not causality constraint has been imposed. We get results that are always within the one sigma Poissonian error of theoretical one $\langle\Psi\rangle_{3D,\ R,\ T=3\tau_0}$.

References

Aguilar, M., Aisa, D., Alpat, B., et al. 2015, Physical Review Letters, 114, 171103
Bernard, G., Delahaye, T., Keum, Y.-Y., et al. 2013, A&A, 555, A48
Bernard, G., Delahaye, T., Salati, P., & Taillet, R. 2012, A&A, 544, A92
Blasi, P. & Amato, E. 2012, JCAP, 1201, 011
Delahaye, T., Lavalle, J., Lineros, R., Donato, F., & Fornengo, N. 2010, A&A, 524, A51
Donato, F., Fornengo, N., Maurin, D., Salati, P., & Taillet, R. 2004, Phys. Rev. D, 69, 063501
Evoli, C., Gaggero, D., & Grasso, D. 2015, JCAP, 1512, 039
Giesen, G., Boudaud, M., Génolini, Y., et al. 2015, JCAP, 1509, 023
Higdon, J. C. & Lingenfelter, R. E. 2003, ApJ, 582, 330
Kachelrieß, M., Neronov, A., & Semikoz, D. V. 2015, Physical Review Letters, 115, 181103
Kappl, R., Reinert, A., & Winkler, M. W. 2015, JCAP, 1510, 034
Lagutin, A. & Nikulin, Y. A. 1995, Soviet Journal of Experimental and Theoretical Physics, 81, 825

Lavalle, J., Maurin, D., & Putze, A. 2014, Phys. Rev., D90, 081301
Lee, M. 1979, The Astrophysical Journal, 229, 424
Lévy, P. 1925, Calcul des probabilités (Gauthier-Villars)
Mandelbrot, B. 1960, International Economic Review, 1, 79
Nolan, J. P. 2012, Stable distributions, Vol. 1177108605 (ISBN)
Serpico, P. D. 2015, in Proceedings, 34th International Cosmic Ray Conference (ICRC 2015)
Tomassetti, N. & Donato, F. 2015, ApJ, 803, L15
Uchaikin, V. V. & Zolotarev, V. M. 1999, Chance and stability: stable distributions and their applications (Walter de Gruyter)
Wolfram Research, Inc. 2016, Mathematica 11.0
Yoon, Y. S., Ahn, H. S., Allison, P. S., et al. 2011, ApJ, 728, 122